Microfluidics and Nanofluidics (2020) 24:10
https://doi.org/10.1007/s10404-019-2313-z

RESEARCH PAPER

Electro-fluidic timer for event control in paper-based devices

Anna Llorella[1] · Marina Navarro-Segarra[1] · Irene Merino-Jiménez[1] · Juan Pablo Esquivel[1] · Neus Sabaté[1,2]

Received: 23 July 2019 / Accepted: 16 December 2019 / Published online: 31 December 2019

Abstract
In this paper, we present a simple yet smart electro-fluidic platform that enables automatic time control in a very affordable and simple manner. The system is based on the electric detection of a fluid front when it crosses a particular area of a paper strip. The detection can be used to trigger the sequential activation or deactivation of different electronic modules (heating of molecular diagnostics, time interval detection, or readout of test results) with an accuracy within the range of minutes. The whole system is implemented with a few number of discrete electronic components such as transistors, resistors and capacitors that, if required, can be totally fabricated using printed electronics technology. This platform opens new possible applications for paper-based point-of care (POC) diagnostic devices and enables the possibility of these devices to introduce time control functions without the need for any external instrumentation and human action.

Keywords Paper microfluidics · Fluidic switch · Paper capacitor · Timer · Electro-fluidic

1 Introduction

The development of portable point-of-care (POC) devices and lab-on-a-chip systems has become a field of interest in the recent years due to their capability to ease global health problems, in particular early diagnosis (Chin et al. 2007; Sia and Kricka 2008). The 'Grand Challenges for Global Health" report from the Bill and Melinda Gates Foundation and the National Institutes of Health (NIH) identified more than a decade ago disease diagnosis and patient monitoring as global priorities. It is an acknowledged consensus that effective diagnosis at the point-of-care requires devices to be inexpensive, easy-to-use, rapid, and instrument-free (Zarei 2017). In this sense, microfluidic paper-based analytical devices based on colorimetric detection are one of the most promising candidates (Yetisen et al. 2013). Their low cost, simplicity, and flexibility make them a solid starting point for the development of new solutions to affordable diagnostics in developing economies (Yang et al. 2014). The intense research in paper-based diagnostics in the last decade has focused on enhancing sensitivity, minimizing batch-to-batch variation and increasing multiplexing capability of these devices (Hu et al. 2014; Tian et al. 2016; Wang et al. 2016). However, one of the pending challenges of this approach is the difficulty to obtain signal quantification in an unambiguous and reliable way (Han et al. 2016; Wong et al. 2012). Generally, colorimetric tests are limited to binary answers (yes/no) or semi-quantified results that rely on color intensity interpretation by the user. In this sense, the introduction of digital means to perform signal interpretation of the test intensity colors has led to significant improvements of test sensitivity and compliance (Delaney et al. 2011; Wang et al. 2015; Yu et al. 2011). This approach requires an external reader to both record images and analyze the result and today, there is a growing trend that mobile phones are excellent ready-to-use, ubiquitous and affordable apparatus (Vashist et al. 2015; Zengerle et al. 2013). Nevertheless, optical detection with smart phone cameras presents some hurdles that prevent its massive adoption in the diagnostics arena. Besides their sensitivity to image resolution and lighting conditions, colorimetric assays are mostly time dependent, which introduces an uncertainty factor that decreases their effectiveness. Before the paper assay can be submitted to the smartphone camera interpretation, the device may require buffer addition, sample heating,

✉ Anna Llorella
anna.llorella@imb-cnm.csic.es

[1] Instituto de Microelectrónica de Barcelona, IMB-CNM (CSIC), Campus UAB, C/dels Til·lers, Campus Universitat Autònoma de Barcelona (UAB), 08193 Bellaterra, Barcelona, Spain

[2] Catalan Institution for Research and Advanced Studies (ICREA), Passeig Lluís Companys 23, 08010 Barcelona, Spain

reactant mixing or incubation time. Generally, time control and sequence of events is performed with external timers that depend on human action, which increases errors during testing (Lewis et al. 2012; Martinez et al. 2008; Zhang et al. 2014). In this regard, issues like sequential reactant delivery, mixing or separation have been successfully solved with passive capillary paper networks (Anderson et al. 2019; Lutz et al. 2013; Toley et al. 2013). However, sequential control of functions requiring the activation of electrical modules is still performed with complex microprocessors that in the paper-based devices scenario are clearly oversized in terms of functionality and cost.

In this paper, we present a simple yet smart electro-fluidic platform that enables automatic time control for sequential event triggering in a very affordable and simple manner. The system is based on the electric detection of a fluid front when it crosses a particular area of a paper strip. The detection can be used to trigger the sequential activation or deactivation of different electronic modules (heating of molecular diagnostics test, time interval detection, or readout of test results) with an accuracy within the range of minutes. The whole system is implemented with a few number of discrete electronic components such as transistors, resistors and capacitors that, if required, can be totally fabricated using printed electronics techniques (Kim et al. 2017; Mattana et al. 2017). The platform opens new possible applications for paper-based POC diagnostic devices and enables the possibility of these devices to introduce time control functions without the need of any external instrumentation and human action.

2 Electro-fluidic activation and deactivation working principle

The system bases its working principle on the arrival of a fluid front inside a paper strip and its effect on the change of permittivity of the paper matrix. This change is detected by placing two metallic and planar electrodes in contact with the paper strip. These electrodes, which are placed in parallel, generate a capacitive behavior between them. The value of the built-up capacitor depends on the geometry of the electrodes, the distance between them and the properties of the dielectric media, where they are embedded (Olthuis et al. 1995). Figure 1 shows a sketch of the capacitors built-up in a porous paper matrix and the lines of the electrical field established between the electrodes. The value of capacitance will change from C_{dry} to C_{wet} upon the arrival of the fluid front due to the change of ε_{rd} to ε_{rw}. The geometrical factors (GF) are constant in both cases.

This change in capacitance can be used as a physical trigger able to enable or disable specific electronically driven functions in a point-of-care device by implementing a smart but simple circuit strategy. Figure 2 shows the schematics of activation and deactivation circuits proposed in this work. The activation circuit consists of connecting in series one reference capacitor (C_{ref1}) to the paper built-up capacitor C_1 in series. Then, the voltage generated by a power source V_{source} connected to the system will be distributed between them according to their capacitance value. As it will be later shown, the paper capacitor will experience an increase in capacitance when the fluid front reaches the electrodes. This change will redistribute the voltage provided by V_{source} by causing an increase in the voltage registered at V_{switch}. Change in V_{switch} can be used to set a MOSFET transistor (Q_1) in conducting state, allowing the current to flow from source to drain and activate a particular electronic component (DEVICE) connected to it. In this configuration—and assuming that a p-type transistor is used-, the value of the reference capacitor has to be selected so the transistor remains closed (off-state) when $C_1 = C_{dry}$ and opens (on-state) when $C_1 = C_{wet}$. The value of C_{ref1} has to be carefully selected so it fulfills the following requirements:

Limit situation:

$$V_{switch} = \frac{V_{source} \cdot C_1}{C_1 + C_{ref1}} = V_{threshold}. \quad (1)$$

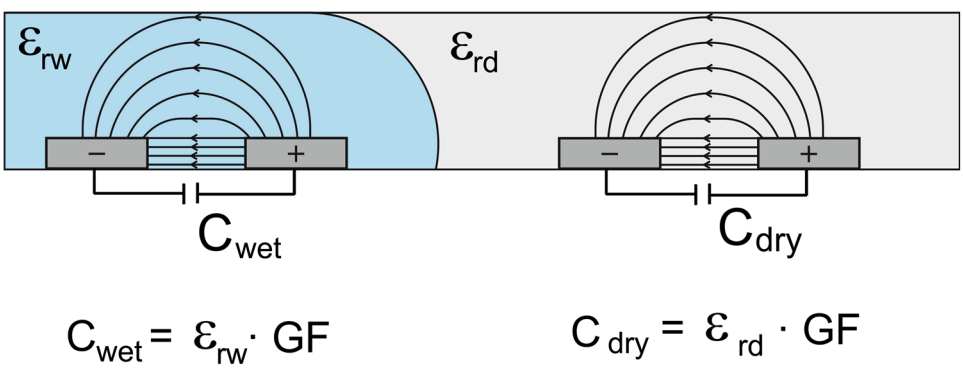

Fig. 1 Lateral view of the planar electrodes and the electric field formed between them. The expression of the capacitance generated in each situation

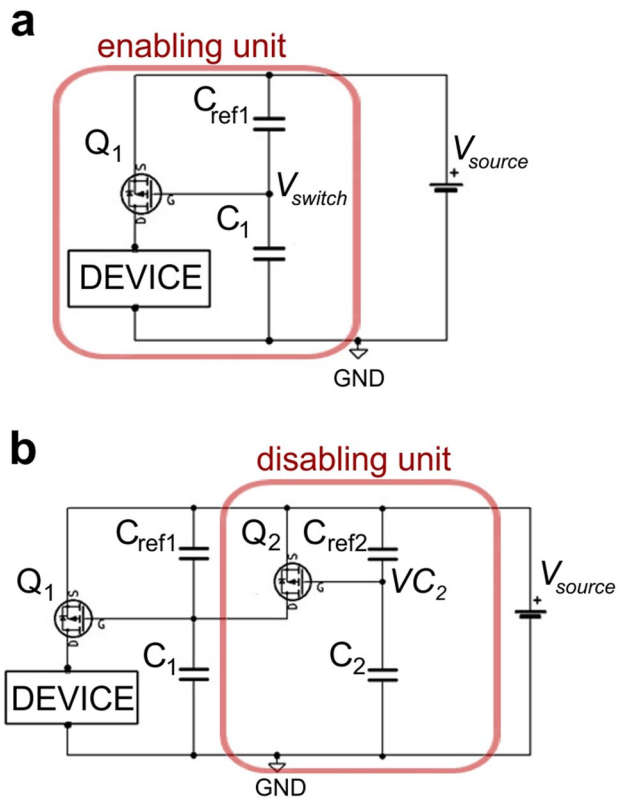

Fig. 2 Schematics of **a** enabling and **b** disabling units

Dry state:

$$V_{\text{switch}} < V_{\text{threshold}}, \tag{2}$$

$$C_{\text{ref1}} > C_{1\text{dry}} \frac{V_{\text{source}} - V_{\text{threshold}}}{V_{\text{threshold}}}. \tag{3}$$

Wet state:

$$V_{\text{switch}} \geq V_{\text{threshold}}, \tag{4}$$

$$C_{\text{ref1}} \leq C_{1\text{wet}} \frac{V_{\text{source}} - V_{\text{threshold}}}{V_{\text{threshold}}}. \tag{5}$$

Requirement condition:

$$C_{1\text{dry}} \frac{V_{\text{source}} - V_{\text{threshold}}}{V_{\text{threshold}}} \leq C_{\text{ref1}} \leq C_{1\text{wet}} \frac{V_{\text{source}} - V_{\text{threshold}}}{V_{\text{threshold}}}. \tag{6}$$

It is possible to switch off the module connected by the enabling unit described above by adding a disabling unit consisting of an additional paper built-up capacitor (C_2), a reference capacitor (C_{ref2}) and a p-type MOSFET transistor (Q_2). The schematics of the disabling unit are depicted in Fig. 2b. In this configuration, when the built-up capacitor voltage (VC_2) decreases due to the arrival of the fluid front, transistor Q_2 allows current to flow from source to drain. This causes the reference capacitor C_{ref1} to discharge and drop its voltage to zero, which at the same times makes transistor Q_1 disable the connection of the particular electronic component (DEVICE).

3 Experimental section

3.1 Chemicals, materials, and processes

Polyethylene naphthalate (PEN) from DuPont (Wilmington, Delaware, USA) was used as a substrate for all the devices presented. The gold nanoparticles ink Drycure Au-JB from C-INK Co., Ltd (Okayama, Japan) was used for the fabrication of the fluidic capacitor. The silver ink from DuPont PE-410 (DuPont, Wilmington, DE, USA) was used for the conductive tracks that define the electronic circuit presented. Both inks were inkjet printed using a Cera Printer X-Series (Ceradrop, Limognes, France).

After that, adhesive silver ink EPO-TEK H20E from Epoxy technology, INK (Massachusetts, USA) was used for the hybridization of the SMD electronic components (Farnell element 14, Barcelona, Spain).

Whatman 1 cellulose paper from GH Healthcare (USA) was used to define the microfluidic matrix placed on top of the fluidic capacitor. A phosphate buffer solution with blue dye (Erioglaucine) from Sigma Aldrich is used for filling the paper matrix during the activation of the electro-fluidic units. Finally, the assembly of the different modules of the devices was designed using CorelDraw software (Corel, Ottawa, ON, Canada) and fabricated using pressure sensitive adhesives (PSA) from Adhesive Research (Pennsylvania, USA). The plastic and paper materials were cut using a CO_2 laser (Mini 24, Epilog Laser, Golden, CO, USA). Paper-based batteries from Fuelium (Barcelona, Spain) were used as power source in the stand-alone prototype.

3.2 Characterization

An impedance analyzer, model 4192A (Hewlett Packard), was used for the characterization of the fluidic capacitor. The electronic validation of the electro-fluidic units was performed using a semiconductor parameter analyzer (Agilent 4155B, Agilent Technologies, California, USA).

The optical characterization of the liquid flow along the paper strip was performed by taking five photographs per second with a webcam (C920 Logitech, Fremont, CA, USA), which was controlled by the software "VideoVelocity Time-Lapse Capture Studio" (CandyLapse, Vancouver, BC, Canada). The photographs analysis was performed using the software package "ImageJ" (US National Institutes of Health, Bethesda, Maryland, USA). The electronic

validation was performed using a data acquisition module (DAQ), NI USB-6009 (National Instruments, USA).

4 Results and discussion

This section describes the design and characterization of the single paper-based built-up capacitors, the enabling and disabling units and a microfluidic platform that allows connecting and powering different sections of an electronic system in a predetermined sequence.

4.1 Characterization of paper-based built-up capacitors

Physical realization of the built-up capacitors has been implemented by inkjet printing several pairs of gold electrodes of 10 mm × 1 mm with a separation of 300 µm on a PEN substrate. Then, a 2 mm-wide paper strip was placed on top of the electrodes setting a contact area of 2 mm^2 with the electrode bands. The paper strip was then covered with a PSA to ensure close contact between the paper strip and the electrodes. The capacitance values between the gold electrode pairs were measured in dry and wet conditions. Wet conditions were achieved by saturating the paper matrix with a colored 100 mM phosphate buffered saline (PBS) solution that mimics a biological fluid. (Abdalla et al. 2010). Figure 3 shows the obtained results between frequencies from 0.0001 to 400 kHz for an electrode pair. The capacitance values corresponding to the dry state of the built-up capacitor range from 0.1 to 0.2 pF. In contrast, the capacitance measured in wet conditions decreases from 90 nF at very low frequencies to 10 pF at 400 kHz. The decrease of capacitance of aqueous media at increasing frequencies is due to the limitation of ion mobility, as ionic species dissolved in water are unable to follow the fast changes in the electric field applied between the capacitor electrodes (Angulo-Sherman and Mercado-Uribe 2011; Rafik et al. 2007).

As the paper strip volume is considered to be constant along the experiment, differences between the capacitance values in wet and dry states can be directly related to the change of permittivity in the paper matrix (Eq. 7):

$$\frac{C_{\text{dry}}}{C_{\text{wet}}} = \frac{\varepsilon_{\text{r,dry}}}{\varepsilon_{\text{r,wet}}}. \tag{7}$$

At high frequencies, the capacitance ratio between wet and dry paper approaches to the ratio 1:80 reported for air and aqueous media (Schwan et al. 1976), whereas at low frequencies, this ratio increases exponentially, reaching a factor of four orders of magnitude at 0.0001 Hz. This ratio does not vary significantly within the range of ionic conductivities of body fluids (0.5–10 mS cm^{-1}), which allows the electro-fluidic strategy to be implemented in many diagnostic applications.

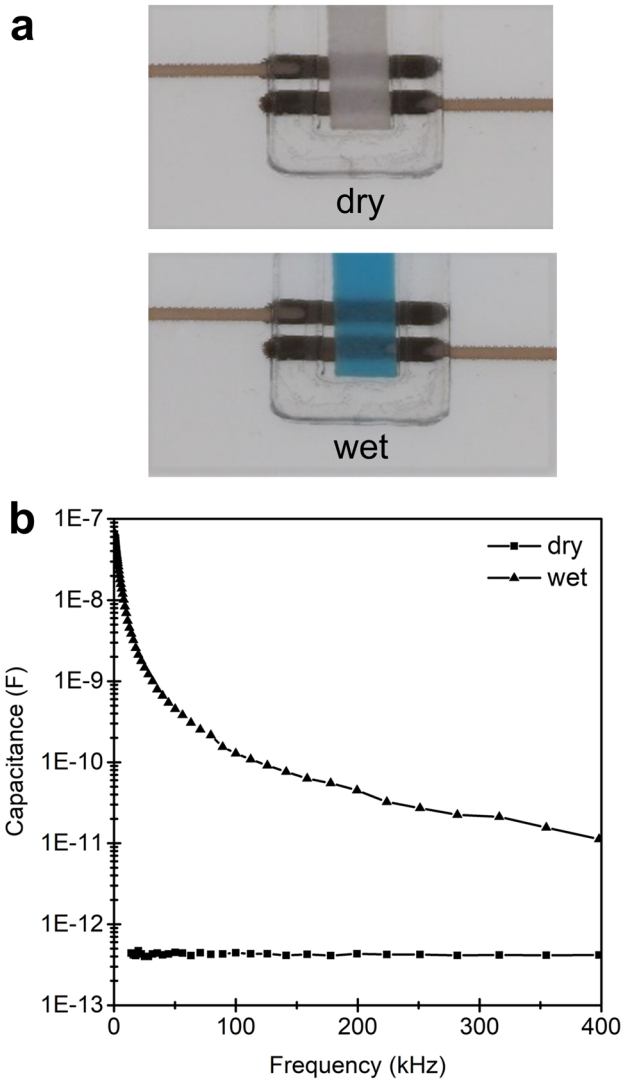

Fig. 3 **a** Photographs of the printed gold electrodes covered by a paper strip in dry and wet conditions. **b** Capacitance values obtained between the pair of electrodes using an impedance analyzer along frequency in both conditions

4.2 Assembly and characterization of single electro-fluidic units

The measured relationship between capacitance values of dry and wet states allowed us the selection of a suitable value of C_{ref} so requirement condition (6) is fulfilled. C_{ref} selection will also be conditioned to the voltage to be applied on the DEVICE element of the circuit. As an example, we have set V_{source} to 1 V and selected a PMOS transistor with a $V_{\text{threshold}}$ of approximately 0.5 V. As the enabling/disabling functions of the unit are to be operated in the low frequency

domain, C_{ref} suitable values range from 0.2 pF to 90 nF. In this case, a ceramic capacitor of 6.8 nF was selected. These elements were hybridized onto a PEN substrate containing inkjet-printed silver tracks and a paper capacitor (C_1). The DEVICE element was implemented with a resistor of 100 KOhms. Figure 4a shows a basic enabling unit.

The unit was set under operation by adding a drop of 5 µL of PBS on the capacitor paper matrix. Both the paper capacitor (C_1) and the reference capacitor (C_{ref}) voltages were monitored during operation. As the results shown in Fig. 4b, before the addition of the fluid the voltage provided by the source (1 V in this case) drops on the paper capacitor, while the voltage drop in the reference capacitor is negligible. Upon the addition of the fluid, voltage drops invert due to the drastic change of C_1 capacitance. This change in voltage is detected by the transistor that turns its state from off- to on-states and enables the current flow through the resistor.

4.3 Development of sequential activation electro-fluidic units

The capillary flow that is established when a fluid wets a paper matrix has been extensively reported in the literature (Ahmed et al. 2016); flow rate depends on several factors such as the paper matrix composition, paper pore size and fluid viscosity (Songok and Toivakka 2016). In this section, we have taken advantage of the progression of the capillary fluid front to develop a platform that enables the sequential activation of a series of electro-fluidic units. The platform, which is shown in Fig. 5a, consists of a PEN substrate, where several pairs of inkjet-printed gold electrodes are connected with a single paper strip. In this configuration, a paper built-up capacitor is established between two electrodes. A layer

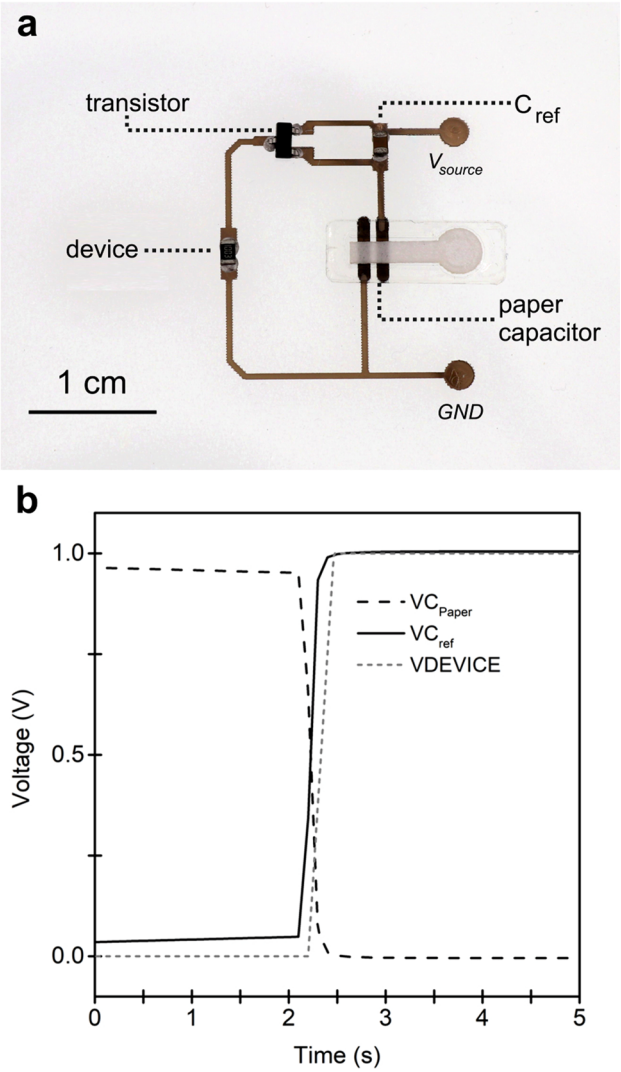

Fig. 4 **a** Photograph of the basic unit fabricated. **b** The evolution of the voltage in the reference capacitor (C_{ref}), in the fluidic capacitor (C_1), and in the DEVICE element during the operation of the platform

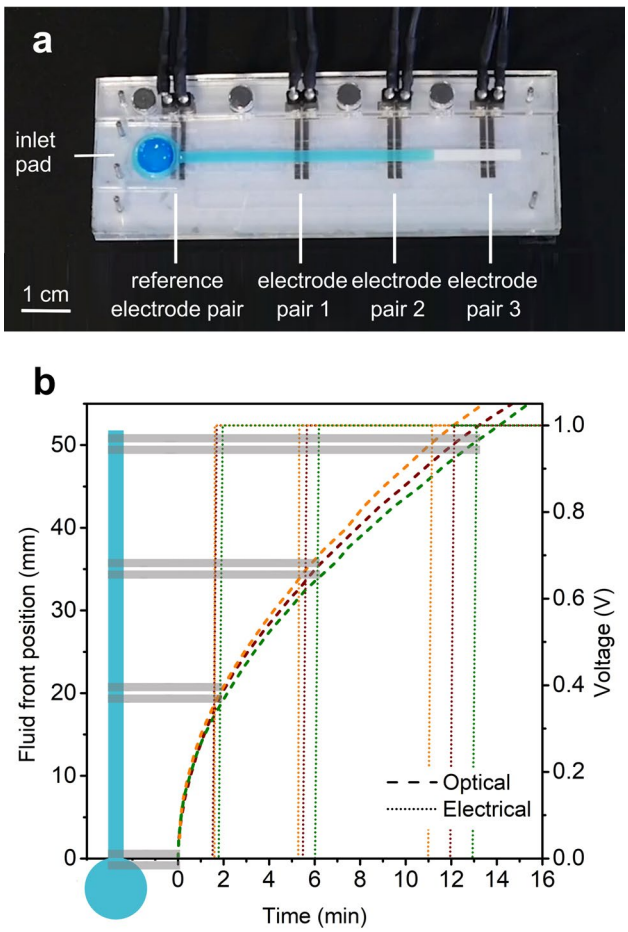

Fig. 5 **a** Platform fabricated for the timing characterization function. **b** Results obtained from the advanced of the fluid along the paper strip detected optically and electronically, each color corresponds to a different tested platform

of PSA material is used to hold and cover the paper along its length, leaving only an inlet pad exposed to air. A PMMA jig is used to define a liquid container at the inlet pad and hold the pins that provide electrical access to the gold electrodes. Characterization of the fluid progression was performed by adding 40 µL of a colored PBS solution in the inlet pad. The fluid front movement along the paper strip was registered with a camera operated at 5 frames per second. The paper capacitors were connected to different activation units like the one shown in the previous section. The units were operated at 1 V and a Data Acquisition (DAQ) module was used to monitor the voltage being applied to the DEVICE element of each unit. To assess the reproducibility of the platform, the experiment was performed three times. Figure 5b shows the position of the fluid front on the left vertical axis and the voltage applied to the different DEVICE elements on the right axis versus time. Right axis depicts the voltage being applied to the different DEVICE elements. The horizontal bars of the graph represent the gold electrode pair's position on the paper strip. It can be observed that the voltage applied to the DEVICE elements increases from 0 to 1 V when the fluid front position reaches the electrode pair of the built-up capacitor connected to their corresponding activation unit.

In this specific configuration, the platform enables the sequential polarization of different DEVICE elements. In particular, activations take place at around the initial point, and after 2, 6 and 12 min. It can be seen that time dispersion of each event increases with electrode distance from the inlet pad. This phenomenon is due to variability introduced by the hand-made assembly of the platform components, in particular, variations on the pressure applied to PSA layer used to fix the paper strip translates into changes on the flow rate. These changes become more evident as the fluid front progresses along the strip.

4.4 Fabrication and characterization of a stand-alone electro-fluidic timer

The sequential electro-fluidic activation strategy has been used to develop a stand-alone demonstration module. This module, shown in Fig. 6a, consists of a platform containing three LED diodes that are activated sequentially once a fluid sample is added onto an inlet pad. A final LED deactivation step that turns off one of the LED diodes has been added. Voltage supply is provided by a paper battery ("Fuelium—Paper-based batteries," n.d.) that is also activated by the fluid arrival to its paper core. The electronic module schematic is shown in Fig. 6b. In this case, the voltage supply required to turn on the LED components is 2.4 V so two paper batteries—that provide 1.5 V each—had to be stacked in series. However, a voltage divider had to be introduced in parallel to the power source to avoid water electrolysis in the built-up capacitors upon the activation of the unit, where they are integrated. As water electrolysis has a standard potential of − 1.23 V (Standard Hydrogen Electrode), this value sets the maximum potential different that can be applied to the paper capacitor electrode terminals to maintain its capacitive behavior.

All electronic components have been assembled on a single PEN substrate containing inkjet-printed gold electrode pairs and silver conductive tracks. The two paper batteries have been placed at one end of the platform and connected to the electronic circuit. A 40 mm long and 2 mm-wide paper strip connects the different electrode pairs. A PSA layer is used to cover the paper strip and fix it to the substrate.

The module has been activated by adding 90 µL of PBS buffer on the paper battery and 40 µL at the inlet pad of the paper strip. The sequential activation and deactivation of the different units has been assessed by measuring the current flowing through each of the LED diodes upon the module onset. Figure 6c shows the results. Once the fluid wets the inlet pad, the first electrode pair—which is printed next to the inlet area—triggers the first activation unit and LED 1 is connected. After 2 min, the fluid front arrives to the second electrode pair and connects LED 2, whereas LED 3 is connected around 2.5 min later. Finally, after 10 min from the initial module onset, the fluid front reaches the electrodes that trigger the deactivation unit and LED3 is switched off.

5 Conclusions

A low-cost paper-based electro-fluidic platform for time event control has been presented. The approach allows a sequential enabling and disabling of the electronic modules connected to it upon the progression of a capillary flow through a porous paper matrix. The working principle is based on the detection of a change in the paper permittivity when a fluid wets a specific area of a paper and the capacitance change of a built-up capacitor attached to it. A basic unit requires only the integration of a capacitor–transistor pair that could be ultimately, fabricated using printed electronics techniques. The platform can be used as an event/time control system during the operation of an instrument-free paper-based diagnostic device. The working principle has been presented and validated with different prototypes of increasing complexity. The stand-alone device presented in the last section has the potential to be readily implemented with already operative paper-based devices and offers the affordability required by the WHO guidelines.

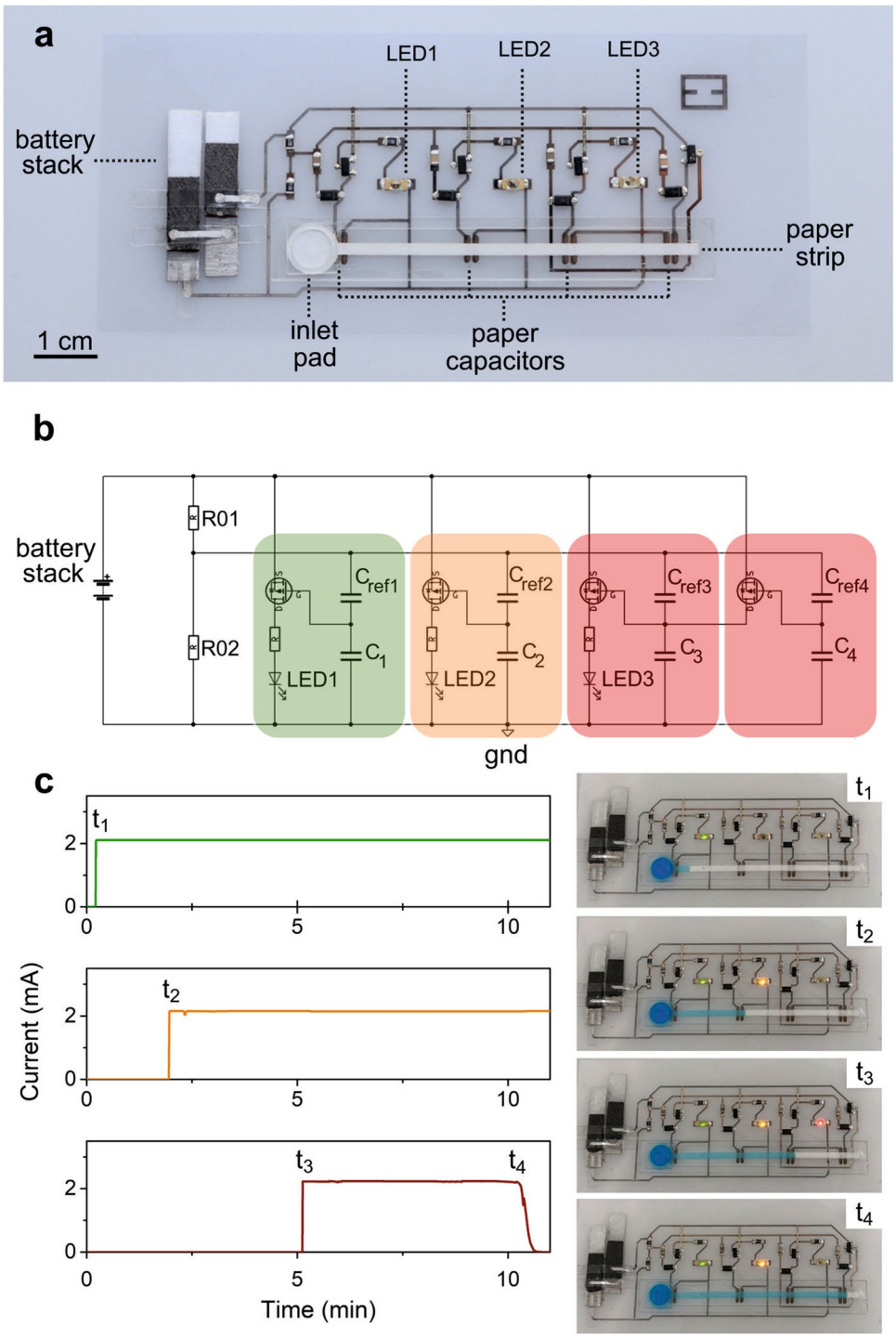

Fig. 6 **a** Photograph of the stand-alone prototype. **b** A scheme of the implemented electronic circuit with its main parts labeled. **c** Current flow through each of the LED diodes during the operation of the prototype and photographs of the prototype during its operation

Acknowledgements R. Escudé and E. Ramón from the ICAS Department at IMB-CNM-CSIC are acknowledged for their technical support in the printed electronic circuits fabrication. N. Sabaté would like to thank the financial support received from the ERC Consolidator Grant (SUPERCELL-GA.648518). I. Merino-Jiménez would like to acknowledge the funding from the European H2020 Framework Programme under the Marie Skłodowska-Curie grant agreement No 665919 (P-Sphere project) and MINAUTO Project (TEC2016-78284-C3-3-R and TEC2016-78284-C3-1-R).

References

Abdalla S, Al-ameer SS, Al-Magaishi SH (2010) Electrical properties with relaxation through human blood. Biomicrofluidics 4:1–16. https://doi.org/10.1063/1.3458908

Ahmed S, Bui MPN, Abbas A (2016) Paper-based chemical and biological sensors: engineering aspects. Biosens Bioelectron 77:249–263. https://doi.org/10.1016/j.bios.2015.09.038

Anderson CE, Buser JR, Fleming AM, Strauch EM, Ladd PD, Englund J, Baker D, Yager P (2019) An integrated device for the rapid and sensitive detection of the influenza hemagglutinin. Lab Chip 19:885–896. https://doi.org/10.1039/c8lc00691a

Angulo-Sherman A, Mercado-Uribe H (2011) Dielectric spectroscopy of water at low frequencies: the existence of an isopermitive point. Chem Phys Lett 503:327–330. https://doi.org/10.1016/j.cplett.2011.01.027

Chin CD, Linder V, Sia SK (2007) Lab-on-a-chip devices for global health: past studies and future opportunities. Lab Chip 7:41–57. https://doi.org/10.1039/b611455e

Delaney JL, Hogan CF, Tian J, Shen W (2011) Electrogenerated chemiluminescence detection in paper-based microfluidic sensors. Anal Chem 83:1300–1306. https://doi.org/10.1021/ac102392t

Fuelium—Paper-based batteries. https://www.fuelium.tech/. Accessed 30 Oct 2019

Han KN, Choi JS, Kwon J (2016) Three-dimensional paper-based slip device for one-step point-of-care testing. Sci Rep. 6:1–7. https://doi.org/10.1038/srep25710

Hu J, Wang SQ, Wang L, Li F, Pingguan-Murphy B, Lu TJ, Xu F (2014) Advances in paper-based point-of-care diagnostics. Biosens Bioelectron 54:585–597. https://doi.org/10.1016/j.bios.2013.10.075

Kim B, Geier ML, Hersam MC, Dodabalapur A (2017) Inkjet printed circuits based on ambipolar and p-Type carbon nanotube thin-film transistors. Sci Rep. 7:1–8. https://doi.org/10.1038/srep39627

Lewis GG, Ditucci MJ, Phillips ST (2012) Quantifying analytes in paper-based microfluidic devices without using external electronic readers. Angew Chemie Int Ed 51:12707–12710. https://doi.org/10.1002/anie.201207239

Lutz B, Liang T, Fu E, Ramachandran S, Kauffman P, Yager P (2013) Dissolvable fluidic time delays for programming multi-step assays in instrument-free paper diagnostics. Lab Chip 13:2840–2847. https://doi.org/10.1039/c3lc50178g

Martinez AW, Phillips ST, Whitesides GM (2008) Three-dimensional microfluidic devices fabricated in layered paper and tape. Proc Natl Acad Sci 105:19606–19611. https://doi.org/10.1073/pnas.0810903105

Mattana G, Loi A, Woytasik M, Barbaro M, Noël V, Piro B (2017) Inkjet-printing: a new fabrication technology for organic transistors. Adv Mater Technol 2:1–27. https://doi.org/10.1002/admt.201700063

Olthuis W, Streekstra W, Bergveld P (1995) Theoretical and experimental determination of cell constants of planar-interdigitated electrolyte conductivity sensors. Sens Actuators B Chem 25:252–256

Rafik F, Gualous H, Gallay R, Crausaz A, Berthon A (2007) Frequency, thermal and voltage supercapacitor characterization and modeling. J Power Sources 165:928–934. https://doi.org/10.1016/j.jpowsour.2006.12.021

Schwan HP, Sheppard RJ, Grant EH (1976) Complex permittivity of water at 25 °C. J Chem Phys 64:2257–2258. https://doi.org/10.1063/1.432416

Sia SK, Kricka LJ (2008) Microfluidics and point-of-care testing. Lab Chip 8:1982. https://doi.org/10.1039/b817915h

Songok J, Toivakka M (2016) Controlling capillary-driven surface flow on a paper-based microfluidic channel. Microfluid Nanofluid 20:1–9. https://doi.org/10.1007/s10404-016-1726-1

Tian T, Wei X, Jia S, Zhang R, Li J, Zhu Z, Zhang H, Ma Y, Lin Z, Yang CJ (2016) Integration of target responsive hydrogel with cascaded enzymatic reactions and microfluidic paper-based analytic devices (μPADs) for point-of-care testing (POCT). Biosens Bioelectron 77:537–542. https://doi.org/10.1016/j.bios.2015.09.049

Toley BJ, McKenzie B, Liang T, Buser JR, Yager P, Fu E (2013) Tunable-delay shunts for paper microfluidic devices. Anal Chem 85:11545–11552. https://doi.org/10.1021/ac4030939

Vashist SK, Luppa PB, Yeo LY, Ozcan A, Luong JHT (2015) Emerging technologies for next-generation point-of-care testing. Trends Biotechnol 33:692–705. https://doi.org/10.1016/j.tibtech.2015.09.001

Wang B, Lin Z, Wang M (2015) Fabrication of a paper-based microfluidic device to readily determine nitrite ion concentration by simple colorimetric assay. J Chem Educ 92:733–736. https://doi.org/10.1021/ed500644m

Wang SQ, Chinnasamy T, Lifson MA, Inci F, Demirci U (2016) Flexible substrate-based devices for point-of-care diagnostics. Trends Biotechnol 34:909–921. https://doi.org/10.1016/j.tibtech.2016.05.009

Wong VL, Pohlmann RA, Ryan US, Noubary F, Jain S, Whitesides GM, Kumar S, Beattie PD, Pollock NR, Rolland JP (2012) A paper-based multiplexed transaminase test for low-cost, point-of-care liver function testing. Sci Transl Med 4:152ra129. https://doi.org/10.1126/scitranslmed.3003981

Yang X, Wu Q, Wang L, Jenkins G, Wang Y, Xie YL, Huang W (2014) Printed electronics integrated with paper-based microfluidics: new methodologies for next-generation health care. Microfluid Nanofluid 19:251–261. https://doi.org/10.1007/s10404-014-1496-6

Yetisen AK, Akram MS, Lowe CR (2013) Paper-based microfluidic point-of-care diagnostic devices. Lab Chip 13:2210–2251. https://doi.org/10.1039/c3lc50169h

Yu J, Ge L, Huang J, Wang S, Ge S (2011) Microfluidic paper-based chemiluminescence biosensor for simultaneous determination of glucose and uric acid. Lab Chip 11:1286–1291. https://doi.org/10.1039/c0lc00524j

Zarei M (2017) Portable biosensing devices for point-of-care diagnostics: recent developments and applications. TrAC Trends Anal Chem 91:26–41. https://doi.org/10.1016/j.trac.2017.04.001

Zengerle R, Schneider EM, Mudanyali O, Vashist SK, Ozcan A (2013) Cellphone-based devices for bioanalytical sciences. Anal Bioanal Chem 406:3263–3277. https://doi.org/10.1007/s00216-013-7473-1

Zhang Y, Zhou C, Nie J, Le S, Qin Q, Liu F, Li Y, Li J (2014) Equipment-free quantitative measurement for microfluidic paper-based analytical devices fabricated using the principles of movable-type printing. Anal Chem 86:2005–2012. https://doi.org/10.1021/ac403026c